

Designing and manufacturing aspherical polystyrene lenses for the terahertz region

A. Shevchik-Sheker^{1*}, V. Zabudsky¹, A. Golenkov¹, S. Dvoretzky²

¹V. Lashkaryov Institute of Semiconductor Physics, NAS of Ukraine, Kyiv, Ukraine

*E-mail: annashsh82@gmail.com

²A.V. Rzhanov Institute of Semiconductor Physics, RAS, pr. Lavrentieva, 13, Novosibirsk, Russian Federation

Abstract. We report on the development of lenses for terahertz vision systems from their design up to manufacturing. Fused deposition modeling was used for assisting the 3D printing manufacturing process. HIP (High Impact Polystyrene) used for printing has high transmittance in the terahertz region and low deformation in the manufacturing process. The comparative analysis of experimental parameters data and the designed ones showed good agreement for the aspherical lenses manufactured. Application of the lenses manufactured to get imaging of some objects at 140 GHz radiation with 32 elements linear detector array has been demonstrated.

Keywords: 3D printing, HIPS, THz lenses, THz region.

doi: <https://doi.org/10.15407/spqeo21.01.083>

PACS 42.15.Eq

Manuscript received 21.02.18; revised version received 14.03.18; accepted for publication 29.03.18; published online 29.03.18.

1. Introduction

Today there exists an ongoing interest in terahertz (THz) technologies. The present-day technological development in the THz range opens new areas of applications in different domains, namely: medicine, security, food control, *etc.* These technologies continue their advance mainly in terms of detectors and sources [1-3]. Also, one of the important tasks in THz instrumentation development is to improve quasi-optic elements for various active THz vision systems.

The majority of THz systems (*e.g.*, pulsed THz systems with photoconductive antennas, continuous wave (CW) photomixer systems) operates basically in the THz spectral range $\nu \sim 0.2 \dots 4$ THz, their output power lies in the range $P < 1 \mu\text{W}$. That's why, as a rule, single detectors are used, and images are acquired using slow raster scanning systems, which takes several minutes to complete relatively small area image, because of the source has a low power. Real-time or close to real-time imaging can be attained using high-power sources such as THz QCLs (Quantum Cascade Lasers) or some others (*e.g.*, the based on, IMPATT (impact ionization avalanche transit-time) diodes, Gunn oscillators, BWOs (Backward Wave Oscillators), *etc.* [4, 5]) and using multielement THz detectors disposed at the plane of irradiation with a relatively large area.

Here, aspheric lenses to focus THz radiation into linear multielement detector array were designed and manufactured on the base of HIPS (High Impact Polystyrene) by 3D printing process. That enabled to get close to real-time imaging of some objects with a multielement linear detector array by using a relatively powerful IMPATT diode and clinotron (variant of the conventional BWO) sources.

2. Designing and manufacturing the terahertz aspherical lenses

The report about aspherical lenses for THz imaging can be found in [6]. There were demonstrated various approaches to the aspherical lens design. One of the most common methods for production is mechanical formation of lenses. These lenses usually have good quality, but they are expensive and hard to produce.

In our early papers [7, 8], we proposed lenses for THz systems based on the refractive aspherical ones. Plastic PTFE (Polytetrafluoroethylene) with ultra-high molecular weight and refractive index of 1.43 was selected as material for lenses. The lenses were processed using a mechanical/polishing lathe, which resulted in a surface roughness less than $30 \mu\text{m}$ ($\sim \lambda/10$). The diffraction-limited system with four identical plano-convex aspherical lenses was obtained. All these lenses were tested using the special stand. For all the lenses, the

focal distance was 70 mm and diameter equal to 60 mm. The calculated and experimental data have close values ($D_{\text{Airy-calc}} = 5.6$ mm, $D_{\text{Airy-meas}} \approx 8$ mm), respectively. Therefore, this type of lenses can be used for THz/subTHz imaging systems [5, 6].

In this work, we used another approach for manufacturing lenses related to the 3D printing capabilities, which reduce manufacturing time, increases cost-efficiency, and allows establishing the full cycle of creating aspherical THz lenses in the one workplace.

The widespread introduction of 3D printing additive technologies, including the method of fused deposition modeling (FDM), allows creating THz optics elements for scientific and technical applications [1-4].

FDM is an additive manufacturing technology that builds parts up layer-by-layer by heating and extruding thermoplastic filament. This technology is clean, low cost and office-friendly.

The FDM printing resolution is of the order of 60...100 μm and depends on the used material. Therefore, this method is perfectly suited to the production of quasi-optical lenses for the THz range, where wavelengths are higher than 1 mm.

Achieving good quality of lenses by FDM 3D printing is not as easy as one could expect. The process depends not only on the 3D model but also on various settings and environmental factors related to the machine itself, its properties and technical condition. Print quality can be significantly improved by knowing how a 3D printer works.

FDM is a process of three-dimensional printing polymeric materials that can be used to produce THz optics. Among the most well-known are: Acrylonitrile butadiene styrene (ABS), Polyactic acid (PLA), Polypropylene (PP), Nylon, BendLay and High Impact Polystyrene (HIPS). For the development of optical elements, important are the refractive indexes and the absorption coefficients of polymer materials for the required THz frequency range. All analyzed materials have a frequency-independent refractive index for applications within the range 0.2 to 1.4 THz [9]. The initial test frequency was 500 GHz [9]. HIPS was chosen for manufacturing, because it is an alternative to highly absorbing PLA, ABS, nylon and HDPE, PP materials that can be deformed during printing. The absorption coefficient in these materials is higher as compared to that of HIPS and grows with increasing the radiation frequency from 140 up to 270 GHz (see Table 1). HIPS has the refractive index value $n = 1.561$ [9]. The 140 and 270 GHz absorption coefficients were determined as being 0.1 and 0.5 cm^{-1} for HIPS, respectively [9].

Various types of lenses can be used in THz vision systems, and one of the promising solutions is to use complex (aspherical) surfaces, which helps to reduce aberrations and losses, as well as to diminish the number of lenses in the system to minimize its weight and manufacturing costs.

We propose cylindrical lenses made using 3D printing for applications requiring one-dimensional shaping of a light source such as a line of detectors.

Table 1. Parameters of some materials for 3D printing at 140 and 270 GHz [9].

Material	Sample thickness (mm)	Refractive index n , 140 GHz	Refractive index n , 270 GHz	Absorption coefficient (cm^{-1}), 140 GHz	Absorption coefficient (cm^{-1}), 270 GHz
ABS	1	1.57	1.57	2	3
PLA	1	1.89	1.89	1	6
Nylon	1	1.72	1.72	0.5	4
HIPS	5	1.561	1.561	0.5	0.5

Two types of optical systems for focusing radiation to point or to line were designed and used in systems with a linear array of detectors. Angular dimensions associated with the horn antenna parameters ($\omega/2 = 14^\circ$) and the image quality requirements close to the diffraction limit were taken as initial conditions for the design.

Different diameters of lenses were chosen to focus radiation into different line sizes, namely: $D = 50$ mm and $D = 80$ mm.

The Zemax program was used for calculations of the optical system. This software has a wide range of options to create and optimize optical systems by using ray tracing. In general, Zemax operates in the geometrical optics approximation, and diffraction effects are calculated in a simple approximation or with a limited number of optical surfaces. The focal length and conic constant k were fitted using the least squares method after modeling the optical system in Zemax to maximize a signal power from the source to detector.

The longitudinal coordinate z ('arrow deflection' of surface) was considered as

$$z = \frac{c \cdot r^2}{1 + \sqrt{1 - (1+k) \cdot c^2 \cdot r^2}}, \quad (1)$$

where r is the distance from the main lens axis, c – inverse radius of curvature of the opposite surface, k – conic constant, which is equal to the square of the eccentricity taken with a minus sign.

The following parameters were obtained: curvature radius of front (+) and rear (–) surfaces was $1/c = 35$ mm, conic constant was $k = -2.06$ (hyperboloid second order surface), focal length $-f = 80$ mm for the lens with $D = 50$ mm; curvature radius of front (+) and rear (–) surfaces $-1/c = 65$ mm; conic constant $-k = -2.6$ (second order surface – hyperboloid), focal length $-f = 125$ mm for the lens with $D = 80$ mm.

The point spread function (PSF) and full-width at half-maximum (FWHM) are often used to estimate optical system quality.

The settings can help to start trying to improve the quality of 3D printed parts. It is necessary to consider that different brands and colors of filaments can also differ in print settings to get the same appearance. Also, various printers can be slightly different, and how they are maintained can have an effect on quality.

The printer Creator Flashforge Pro have been used for making lenses from HIPS, thread by MonoFilament

Table 2. The optimal setting parameters for printing polystyrene lenses.

Temperature of table surface, °C	110
Temperature of nozzle, °C	230
Height of the layers, μm	100
Print speed, mm/min	2100
Plastic filling, %	100
Material blowing	no



Fig. 1. Lenses and fastenings manufactured on the 3D printer.

with the diameter 1.75 mm. We have collected some settings based on our experience, namely: temperature of table surface and nozzle, the height of the layers, print speed and others (see Table 2).

We have passed complete cycle creation of THz lenses including: calculation, 3D simulation to 3D fabrication in one workplace. This approach allows significant reduction of the development time of THz lenses and minimizes their cost.

The printing process of lenses and fastening took approximately three hours. The manufactured parts are shown in Fig. 1.

3. Testing the THz lenses

Fig. 2 shows an experimental setup for evaluating quality of the lenses designed and manufactured.

The THz source based on the IMPATT diode with a conical horn antenna was used as the emitter generating continuous, linearly polarized, essentially monochromatic radiation with the power $P \approx 20$ mW at $f = 140$ GHz. The conical antenna has the following parameters: frequency range is $\nu \approx 110 \dots 170$ GHz, gain is ≥ 20 dBi, waveguide type is rectangular, waveguide size is WR-6, aperture diameter is 27 mm, horn length is 38 mm.

Tunable BWO source operating within the frequency range $f = 128 \dots 152$ GHz and radiation power $P \sim 4 \dots 10$ mW was also used. At 270 GHz, the radiation power from clinotron source was $P \approx 140$ mW, gain was ≥ 20 dBi, the conical antenna aperture diameter was 25 mm, horn length was 45 mm. In all these sources, horn antennas to transmit THz power in free space were used.

The pair of lenses focuses the light into point or line (at detector linear array). This scheme was chosen as the intermediate one for simulating illumination of the object in a spot or line followed by focusing on one or line receivers.

To estimate quality of the lenses, the relative power distribution from sources was mapped by HgCdTe or pyroelectric detectors [10] through the motorized three-coordinate stages displacement (Fig. 1). The output electric signal of detectors was measured using the lock-in amplifier Stanford SR 830. The dynamic range of the system was about 60 dB.

In Figs 3 and 4, we show the XY cross section (at z – the focal plane of the lenses) of the 3D the PSF of the lenses for focusing radiation to point and to line, with $f = 125$ mm, $a = 80$ mm. We show comparison of the computer modeling (c, d) and the experimental results (a, b) the PSF fit through the maximum in x - and y -direction and photographs of the lenses. The FWHM is stated in Table 3.

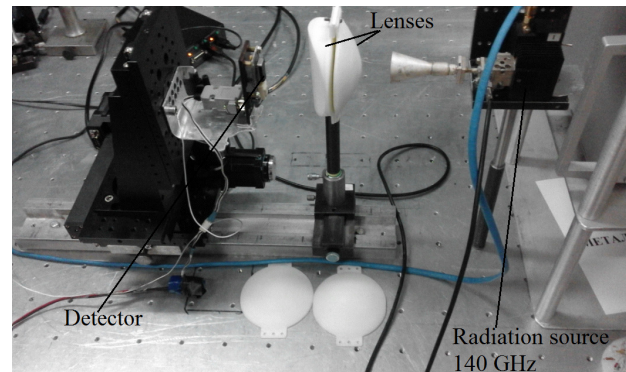


Fig. 2. Experimental setup for testing the lenses with THz source based on IMPATT diode (140 GHz).

Table 3. The full-width at half-maximum of the collimated and focused beam for different type of lenses at frequencies 140 and 270 GHz are shown. Presents the focusing properties of the lenses and compares with calculated results of the beam diameters, calculated using a Gaussian beam. Both lenses focus properties like expected and showing the dimensions of the spots close to the diffraction limit.

A system from two axially symmetric lenses with the aspherical surfaces, $\varnothing = 80$ mm, $f = 125$ mm			
140 GHz		270 GHz	
Calculated FWHM, x/y , mm	Measured FWHM, x/y , mm	Calculated FWHM, x/y , mm	Measured FWHM, x/y , mm
4.5/4.5	4.5/4.4	2/2	2.5/2.5
A system from one axially symmetric lens and one asymmetrical (cylindrical) lens with the aspherical surfaces, $\varnothing = 80$ mm, $f = 125$ mm			
140 GHz		270 GHz	
Calculated FWHM, x/y , mm	Measured FWHM, x/y , mm	Calculated FWHM, x/y , mm	Measured FWHM, x/y , mm
4.5/ image is a line equal to the lens diameter	4.5/10.5	2.5/ image is a line equal to the lens diameter	2.5/5

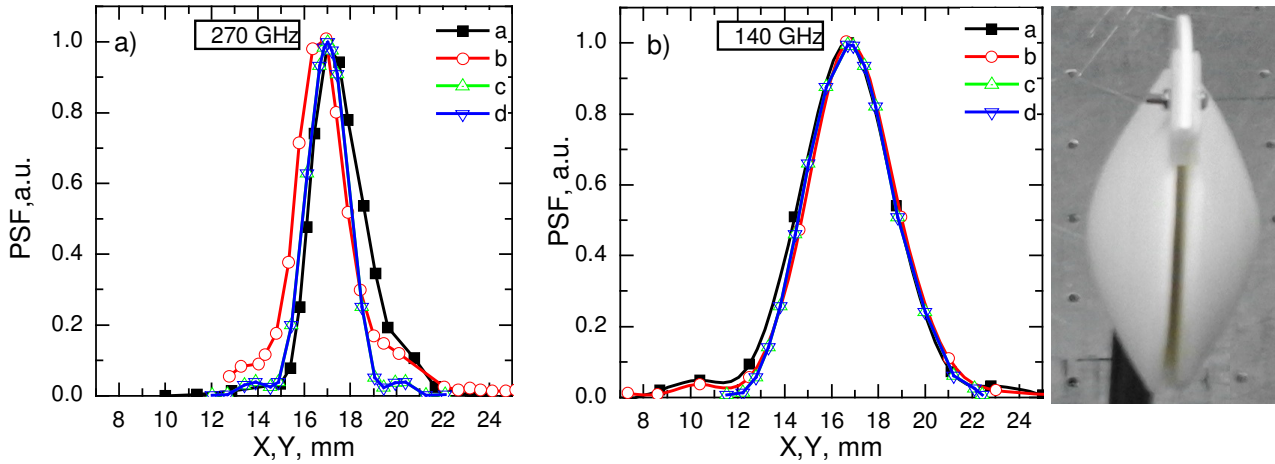


Fig. 3. The system from two axially symmetric lenses with the aspherical surfaces with focal length of 125 mm and diameter of 80 mm. The comparison of the computer modeling (c, d) and the experimental results (a, b) the PSF fit through the maximum in x- and y-direction and photographs of the lenses. The full-width at half-maximum is stated in Table 3.

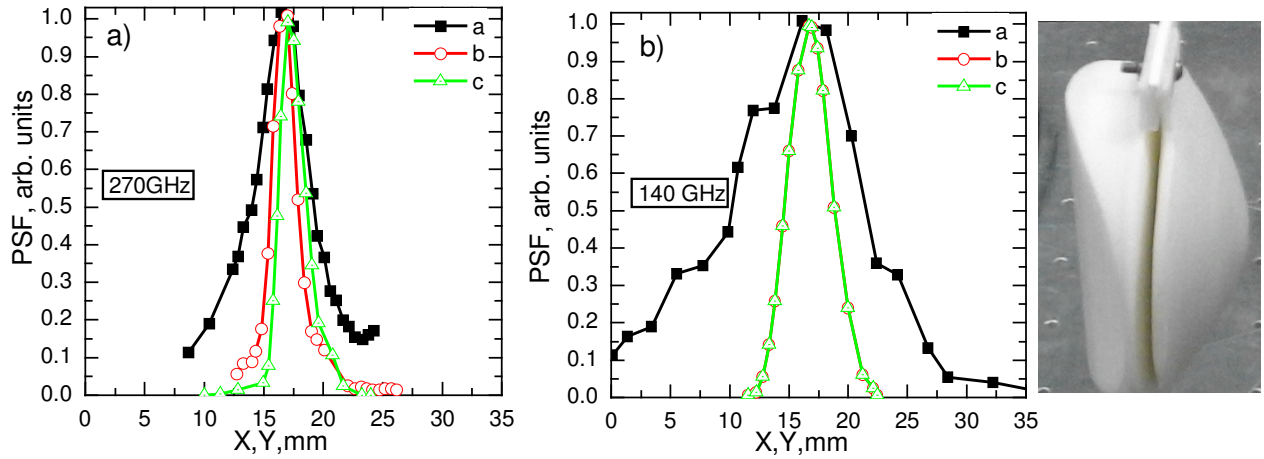


Fig. 4. The system from one axially symmetric lens and one asymmetrical (cylindrical) lens with the aspherical surfaces with focal length of 125 mm and diameter of 80 mm. The comparison of the computer modeling (c) and the experimental results (a, b) the PSF fit through the maximum in x- and y-direction and photographs of the lenses. The full-width at half-maximum is stated in Table 3.

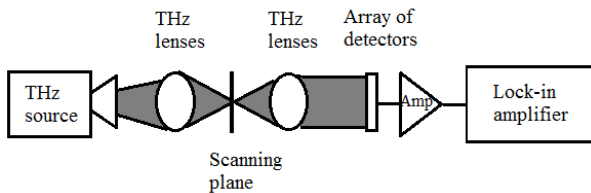


Fig. 5. The block diagram of the optical setup for XYZ scanning of the objects.

The focusing properties are as expected and show spot sizes that are close to the diffraction limit for the system from two axially symmetric lenses. The results of calculations and measurements differ at Y axis due to the source Gaussian radiation, not Lambertian for the system from one axially symmetric lens and one asymmetrical (cylindrical) lens.

The sizes of the FWHM at 140 GHz are bigger than those at 270 GHz almost twice. That corresponds to the

theory that for the same aperture size of the element the spot size depends directly proportional to the frequency.

The THz images were taken using the setup shown in Fig. 5. A narrow parallel beam from the IMPATT diode at 140 GHz was formed using combination lenses. The first pair of lenses from one axially symmetric lens and one asymmetrical (cylindrical) lens focuses the light into the line on the object; the second from two axially symmetric lenses focused it to the 32 elements THz array detectors (silicon field effect transistors). The detector voltage signal was collected using a preamplifier (Amp) and a lock-in amplifier.

Fig. 6 shows the image of objects obtained using the printed lenses from HIPS material in the THz (32 elements THz array of total 80 element array, silicon field-effect transistors, pitch 1 mm) and visible ranges.

The image was obtained for hidden objects behind the plastic foam of the thickness $d = 1$ cm. One can clearly see the different washer, pill, and sugar with sufficient spectral resolution ~ 4.5 mm.

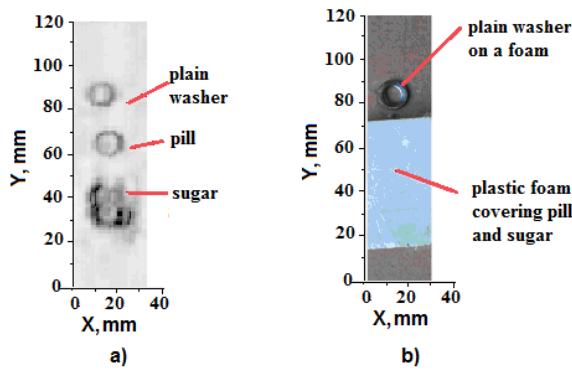


Fig. 6. a) Washer, pill, and sugar that are hidden behind plastic foam of the thickness $d = 1$ cm, b) the same objects in the visible range.

The obtained results confirm the possibility to get high-quality aspherical lenses by using the plastic layering method of 3D printing with close to simulated parameters such as focal lengths and PSF. A quantitative method of determining the quality of this image is calculation of the FWHM and comparison with the experimental data. In our case, they are $\text{FWHM}_{\text{calc.,x/meas.,x}}$ (140 GHz) = 4.5 mm/4.5 mm, $\text{FWHM}_{\text{calc.,y/meas.,y}}$ (140 GHz) = 4.5 mm/4.4 mm) for axially symmetric lenses, $\varnothing = 80$ mm, which provides resolution ~ 4.5 mm. The FWHM is $\text{FWHM}_{\text{calc.,x/meas.,x}}$ (140 GHz) = 4.5 mm/4.5 mm, $\text{FWHM}_{\text{calc.,y/meas.,y}}$ (140 GHz) = 10.5 mm/(image is a line with the length equal to the half lens diameter) for the one axially symmetric lens and one asymmetrical (cylindrical) lens .

4. Conclusions

The possibility of manufacturing relatively good-quality THz lenses from high impact polystyrene material (HIPS) by 3D printing has been shown. It was proposed to use cylindrical lenses for applications requiring one-dimensional shaping of a light source such as a line of detectors. HIPS was chosen for manufacturing THz lenses, because it has advantages compared to highly absorbing PLA, ABS, nylon and HDPE, PP materials that can also be deformed during printing. Images of “hidden in the visible spectrum” objects were obtained with the use of manufactured lenses of sufficient spectral resolution ~ 4.5 mm by using the 140 GHz frequency source. Scanning (with the frame rate ~ 1 Hz) in the direction perpendicular to 32-pixel linear detector array based on silicon field-effect transistors has been carried out.

Acknowledgments

This paper is partly based on researches supported by Volkswagen Project Application No. A115974 “Optoelectronic and transport phenomena in narrow-gap semiconductor structures for terahertz detection”.

References

1. Kai-Erik Peiponen, J. Axel Zeitler, Makoto Kuwata-Gonokami (Eds.), *Terahertz Spectroscopy and Imaging*. Springer, 2013.
2. Squires A.D., Constable E., Lewis R.A. 3D printing of aspherical terahertz lenses and diffraction gratings. *39th Intern. Conf. on Infrared, Millimeter, and Terahertz waves (IRMMW-THz)*, IEEE. P. 1–2.
3. Rachon M., Liebert K., Siemion A., Bomba J., Sobczyk A., Knap W., Coquillat D., Suszek J., Sypek M. Geometrical aberration suppression for large aperture sub-THz lenses. *J. Infrared, Millimeter, and Terahertz Waves*. 2017. **38**, No. 3. P. 347–355.
4. Gallerano G.P., and Biedron S. Overview of terahertz radiation sources. *Proc. 2004 FEL Conf. Triest, Italy, 2004*. P. 216–221.
5. Paul D.J. The progress towards terahertz quantum cascade lasers on silicon substrates. *Laser Photon. Rev.* 2010. **4**, No. 5. P. 610–632.
6. Yat Hei Lo, Leonhardt R., Torres V., Pacheco-Pena V., Rodriguez-Ulibarri P., Navarro-Cia M., Beruete M., Sorolla M., Enghet N. Aspheric lenses for terahertz imaging. *Opt. Exp.* 2008. **16**, No. 20. P. 15991–15998.
7. Sizov F., Tsybrii Z., Zabudsky V., Sakhno M., Shevchik-Shekera A., Smoliiy M., Dieguez E., Dvoretzky S. Possibility of the detection in IR and sub/THz spectral region using MCT thin layer receivers: design of the chip, optical elements and antenna pattern. *IEEE MMS 2015*. Lecce, Italy, 2015, P. 49-52.
8. Sizov F., Tsybrii Z., Zabudsky V., Golenkov O., Petryakov V., Dvoretzky S., Michailov N., Shevchik-Shekera A., Lysiuk I., Dieguez E. Mercury–cadmium–telluride thin layers as subterahertz and infrared detectors. *Opt. Eng.* 2015. **54**, No. 12. P. 127102-1–127102-8.
9. Busch S., Weidenbach M., Fey M., Schafer F., Probst T., and Koch M. Optical properties of 3D printable plastics in the THz regime and their application for 3D printed THz optics. *J. Infrared, Millimeter, Terahertz Waves*. 2014. **35**. P. 993–997.
10. Sizov F., Zabudsky V., Golenkov A., and Shevchik-Shekera A. Mm-wave narrow-gap uncooled hot-carrier detectors for active imaging. *Opt. Eng.* 2013. **52**, No. 3, P. 033203.

Authors and CV



Anna Shevchik-Shekera received the BS and MS degrees in laser and optoelectronic engineering from the National Technical University of Ukraine, Kiev, in 1993 and 1995, respectively. From 2005 to 2008 she was with the Institute of Semiconductor Physics

of NASU as a design engineer, where she was involved in the design of thermal imaging cameras. Since 2008, she has been working as a researcher. Her research interests include infrared and millimeter-wave imaging of active vision systems.

V. Lashkaryov Institute of Semiconductor Physics, NAS of Ukraine, Kyiv, Ukraine
E-mail: annashsh82@gmail.com



Vyacheslav V. Zabudsky received the PhD degree in 1997 on the specialty “Physics of semiconductors and dielectrics” from the National Academy of Sciences of Ukraine. His professional activities are in the fields of infrared microphotoelectronics,

semiconductor low-dimension structures, developing of the testing equipment and methods, investigation of HgCdTe detecting properties, infrared and terahertz detectors and vision systems in these spectral regions. In these areas, he has published more than 50 scientific and technical papers.

V. Lashkaryov Institute of Semiconductor Physics, NAS of Ukraine, Kyiv, Ukraine



Aleksandr G. Golenkov graduated from the physics department of Kyiv State University (1996), and received his PhD degree on the specialty “Physics of devices, elements and systems” (2008). His work experience is in the fields of infrared and microwave

electronics, semiconductor low-dimension structures, testing equipment and methods, information reading and processing methods, investigation of the infrared (MCT) and terahertz (MOSFET) detectors.

V. Lashkaryov Institute of Semiconductor Physics, NAS of Ukraine, Kyiv, Ukraine



Dvoretzkiy Sergey Alekseevich, PhD from the Institute of Semiconductor Physics of Siberian Branch of Academy of Sciences of Russia, 1975. 1969-1995, Institute of Semiconductor Physics, Novosibirsk. Junior scientific researcher (1972), senior scientific researcher (1987), leader of group of MBE

II-VI compound (1988), Head of Laboratory (2012), till now. The basic research is the growth II-VI compound including narrow gap HgCdTe hetero- and nanostructures.

A.V. Rzhanov Institute of Semiconductor Physics, RAS, pr. Lavrentieva, 13, Novosibirsk, Russian Federation